# Use of Inverse Gas Chromatography To Study Binary Polymer−Solvent Systems near the Glass Transition Temperature

**Peter K. Davis,[†] Ronald P. Danner,*[,†] J. Larry Duda,[†] and Ilyess Hadj Romdhane[‡]**

*The Center for the Study of Polymer-Solvent Systems, Chemical Engineering Department, The Pennsylvania State University, University Park, Pennsylvania 16802, and 3M Engineering Systems Technology Center, 3M Center, Bldg 518−1−01 St. Paul, Minnesota 55144-1000*

*Received June 7, 2003; Revised Manuscript Received October 19, 2003*

ABSTRACT: A new model has been developed for inverse gas chromatography experiments for binary polymer−solvent systems. The model includes both bulk and surface effects and has been solved using the method of Laplace transforms. Retention data near the glass transition temperature were collected from the literature and correlated and predicted with the model. Frequently investigators estimate a polymer's glass transition temperature ($T_g$) from the Z-shaped retention data that often occur in this temperature range. The results presented here suggest that there is little or no correlation between the Z-shaped retention diagram and the glass transition temperature. New results are also presented on the origins of the Z-shaped retention diagram and on how a combination of bulk absorption, bulk diffusion, and surface adsorption contribute to it.

## Introduction

Inverse gas chromatography is a commonly used experimental technique to measure sorption and diffusion in polymer solvent systems. The parameter most often measured by this experiment is the retention volume, a parameter that gives information about the thermodynamics of a polymer−solvent system. When the natural logarithm of the retention volume is plotted vs reciprocal temperature, the resulting line is called a retention diagram. Numerous investigators have developed these diagrams for different systems, and many have found a Z-shaped behavior pattern around the glass transition temperature of the polymer.[1−7] An example of this type of retention diagram is shown in Figure 1.

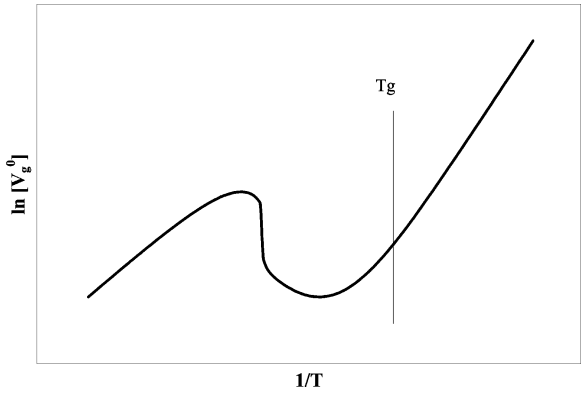


**Figure 1.** Example of a Z-shaped retention diagram.

It has been suggested that this behavior could be used to detect the glass transition. The glass transition is thought to occur at the first deviation from linearity of the retention diagram in the low temperature region. Many investigators have speculated that below the $T_g$ bulk absorption did not occur in the polymer. In this region, it was proposed that only surface adsorption occurred. It was also proposed that the first deviation from linearity indicates the onset of bulk diffusion. To better understand the mechanisms behind the Z-shaped retention diagram, a new model for inverse gas chromatography experiments has been developed. The model has been derived to include both bulk absorption and surface adsorption effects. The model was used to determine the origins of the retention behavior around the polymer's $T_g$.

## Binary Polymer−Solvent System Inverse Gas Chromatography Model

In an inverse gas chromatography experiment, a polymeric stationary phase is placed inside an empty column. A pulse of solvent (called a probe molecule) is injected into this column where it mixes with an inert carrier gas and travels though the length of the column. The raw data collected are the solvent concentration in the carrier gas at the column's outlet as a function of time. The shape of this elution profile gives information about the properties of the polymer−solvent system. The polymeric stationary phase can be inserted into the column by a variety of techniques. The two most typical methods are capillary column inverse gas chromatography (CCIGC) and packed column inverse gas chromatography (PCIGC). In a CCIGC experiment, the inside of a capillary column is coated with a thin film of polymer. In PCIGC, the polymer is coated on support particles. These particles are then packed into the empty column. In either case, to model the solvent's elution profile, it is necessary to identify the various resistances that the solvent pulse encounters as it passes through the column. Here, three dominant mechanisms are identified by which the solvent's retention can be altered. The first is gas phase dispersion due to axial concentration gradients of solvent in the carrier gas. Molecular diffusion in the gas phase is assumed fast such that the gas is well mixed in the radial direction and Taylor dispersion is negligible. Thus, it is necessary to only consider the effect of axial dispersion in the gas phase. The second mechanism is bulk absorption of the solvent by the polymer coating. Finally, solvent elution

* To whom correspondence should be sent. E-mail: rpd@psu.edu. Telephone: 814-863-4814. Fax: 814-865-7846.
[†] The Pennsylvania State University.
[‡] 3M Center.

10.1021/ma0347767 CCC: $27.50 
Published on Web 11/04/2004

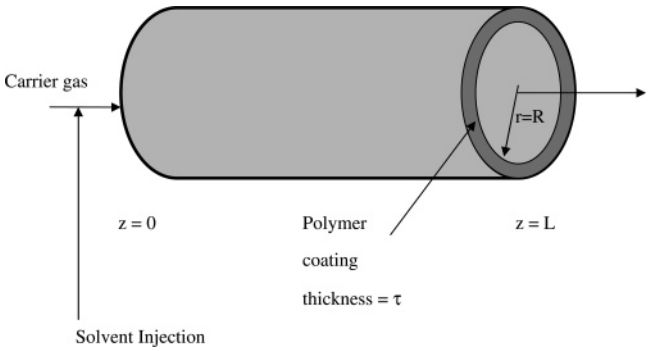


**Figure 2.** Diagram of a capillary column inverse gas chromatography experiment.

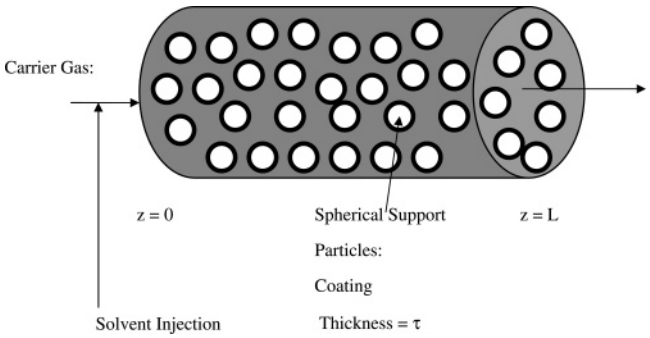


**Figure 3.** Diagram of packed column inverse gas chromatography experiment.

may be retarded because of adsorption onto the gas−polymer interface.

The original IGC model was developed by Macris,[8] who considered only axial dispersion and bulk absorption in a capillary-coated column. In this paper, this model is extended to include adsorption effects and is generalized for either packed column or capillary column IGC. Figure 2 below shows a diagram of the capillary column process, and Figure 3 shows the packed column operation. Figure 4 defines the nomenclature of the radial coordinates for both capillary and packed column IGC.

In the derivation of the governing equations, the following assumptions are made.

1. The entire system is isothermal.

2. For capillary column operation, the polymer coating thickness is much smaller than the column radius. For packed column operation, the polymer coating thickness is much smaller than the support particle radius.

3. Gas phase diffusion is assumed to be sufficiently fast to keep the gas well mixed in the radial direction, making Taylor dispersion insignificant compared to conventional axial dispersion.

4. No pressure drop occurs over the column length.

5. The polymer phase diffusion coefficient is constant over the concentration range of the perturbation.

6. The vapor phase diffusion coefficient is constant.

7. The thermodynamics of bulk absorption into the polymer can be described by a constant partition coefficient.

8. The polymer film has a uniform thickness through the entire column.

9. Diffusion in the polymer phase occurs only in the r direction.

10. The carrier gas is insoluble in the polymer and does not adsorb on any surfaces.

11. Surface adsorption by the solvent is described by a constant surface equilibrium constant over the concentration range of the perturbation.

12. No chemical reactions occur.

13. The partial molar volume of the solvent in the polymer is constant.

14. Swelling of the polymer is insignificant.

15. The solvent injection can be modeled by a simple Dirac $\delta$ function.

With the above assumptions, the continuity equation for the solvent in the polymer phase is:

$$\frac{\partial \rho}{\partial t} = D_{\mathrm{p}} \frac{\partial^2 \rho}{\partial r^2} \tag{1}$$

$$t = 0, \quad \rho = 0 \tag{2}$$

$$r = R, \quad \rho = K_{\mathrm{p}} C \tag{3}$$

$$r = R + \tau, \quad \frac{\partial \rho}{\partial r} = 0 \tag{4}$$

In eqs 1−4, $\rho$ is the mass concentration of solvent in the polymer phase, $D_{\mathrm{p}}$ is the mutual diffusivity of the polymer phase, and $C$ is the mass concentration of solvent in the vapor phase. The $K_{\mathrm{p}}$ parameter is the bulk solvent partition coefficient between the gas and polymer phase. The following dimensionless variables are introduced:

$$\rho' = \frac{\rho}{\frac{K_{\mathrm{p}} C_0 V}{L}} \tag{5}$$

$$C' = \frac{C}{\frac{C_0 V}{L}} \tag{6}$$

$$t' = \frac{tV}{L} \tag{7}$$

$$r' = \frac{r - R}{\tau} \tag{8}$$

$$z' = \frac{z}{L} \tag{9}$$

In eqs 5 and 6, $C_0$ is the strength of the solvent inlet pulse and has units of (g-s/cm$^3$). The carrier gas velocity is defined as $V$. Substituting these variables into eqs 1−4 gives

$$\frac{\partial \rho'}{\partial t'} = \left[\frac{1}{\beta^2}\right] \frac{\partial^2 \rho'}{\partial r'^2} \tag{10}$$

$$t' = 0, \quad \rho' = 0 \tag{11}$$

$$r' = 0, \quad \rho' = C' \tag{12}$$

$$r' = 1, \quad \frac{\partial \rho'}{\partial r'} = 0 \tag{13}$$

In eq 10, $\beta^2 = (V\tau^2/LD_{\mathrm{p}})$. Physically, it can be thought of as the governing dimensionless quantity for mass transport in the polymer coating. Macris has shown that this type of differential equation can be solved using

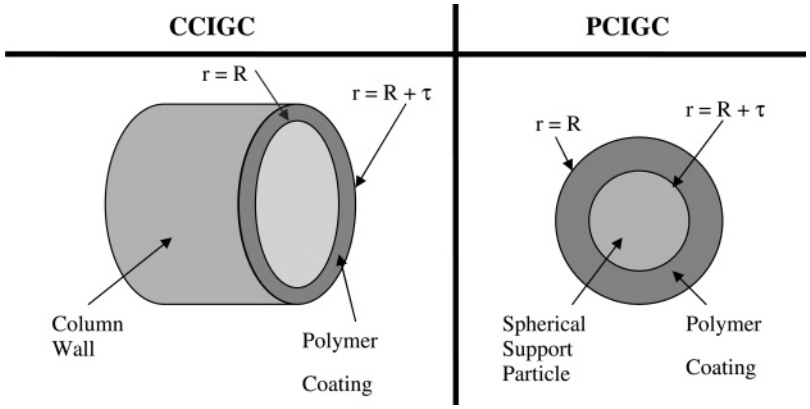


**Figure 4.** Definition of the radial ($r$) coordinates for model derivation.

Laplace transforms. Employing this solution gives

$$Q = \frac{Y}{1 + e^{2\beta\sqrt{s}}} e^{\beta\sqrt{s}r'} + \frac{Ye^{2\beta\sqrt{s}}}{1 + e^{2\beta\sqrt{s}}} e^{-\beta\sqrt{s}r'} \quad (14)$$

Here, $Q(s,r)$ is the Laplace variable for $\rho'(t,r)$ and $Y(s,z)$ is the Laplace variable for $C'(t,z)$. Under the assumptions outlined above, the gas phase solvent species continuity equation is

$$\frac{\partial C}{\partial t} + V\frac{\partial C}{\partial z} = D_g\frac{\partial^2 C}{\partial z^2} + \frac{A_s D_p}{\chi}\frac{\partial \rho}{\partial r}|_{r=R} - \frac{A_s K_s}{\chi}\frac{\partial C}{\partial t} \quad (15)$$

$$t = 0, \quad C = 0 \quad (16)$$

$$z = 0, \quad C = \delta(t)C_0 \quad (17)$$

$$z = \infty, \quad C = 0 \quad (18)$$

In eq 15, $K_s$ is the surface adsorption partition coefficient. Using the dimensionless variables defined in eqs 5−9

$$(1 + \epsilon)\frac{\partial C'}{\partial t'} + \frac{\partial C'}{\partial z'} = \gamma\frac{\partial^2 C'}{\partial z'^2} + \frac{2}{\alpha\beta^2}\frac{\partial \rho'}{\partial r'}|_{r'=0} \quad (19)$$

$$t' = 0, \quad C' = 0 \quad (20)$$

$$z' = 0, \quad C' = \delta(t') \quad (21)$$

$$z' = \infty, \quad C' = 0 \quad (22)$$

Here, the following dimensionless groups have been introduced:

$$\alpha = \frac{2\chi}{K_p \tau A_s} \quad (23)$$

$$\gamma = \frac{D_g}{VL} \quad (24)$$

$$\epsilon = \frac{A_s K_s}{\chi} \quad (25)$$

In these equations, $\chi$ is the void fraction of the column and is defined as the volume of the column filled with gas divided by the empty column volume. The $A_s$ parameter is the exposed polymer surface area per volume of empty column. For CCIGC, $\chi$ is very close to unity and $A_s$ = (2/column radius). For PCIGC, they take on their appropriate values depending on the packing. For CCIGC, $D_g$ is the mutual binary diffusivity for the gas phase, while for PCIGC, it is an effective diffusivity that depends both on the tortuosity and the axial mixing created by the packing. This equation can also be solved in the Laplace domain:

$$Y = \exp\left\{z'\left(\frac{1}{2\gamma} - \sqrt{\frac{1}{4\gamma^2} + \frac{2\sqrt{s}}{\alpha\beta\gamma}\tanh(\beta\sqrt{s}) + \frac{(1+\epsilon)s}{\gamma}}\right)\right\} \quad (26)$$

It is desired to model the solvent gas concentration at the end of the column ($z' = 1$) since this is where the detector is located. The solution at the column exit is

$$Y = \exp\left\{\frac{1}{2\gamma} - \sqrt{\frac{1}{4\gamma^2} + \frac{2\sqrt{s}}{\alpha\beta\gamma}\tanh(\beta\sqrt{s}) + \frac{(1+\epsilon)s}{\gamma}}\right\} \quad (27)$$

It is very difficult to analytically invert eq 27 back into the time domain, so solution of the model was accomplished by numerical inversion using a fast Fourier transform (FFT) algorithm.

## IGC Data Analysis

The most common parameter measured from IGC experiments is the specific retention volume ($V_g^0$) at reference temperature $T_0$:

$$V_g^0 = \frac{T_0}{T}\frac{V_N}{M_p} \quad (28)$$

In this equation, $V_N$ is the net retention volume and $M_p$ is the mass of polymer in the column. The reference temperature, $T_0$, is usually taken to be 273.15 K, and $T$ is the column temperature. The net retention volume is defined as

$$V_N = F(t_r - t_c)j = \frac{L}{V}F(t'_r - t'_c)j \quad (29)$$

$$j = \frac{3}{2}\frac{\left(\frac{P_i}{P_o}\right)^2 - 1}{\left(\frac{P_i}{P_o}\right)^3 - 1} \quad (30)$$

Here, $F$ is the volumetric flow rate of the carrier gas and $j$ is a correction for the pressure drop in the column.[12] The inlet and outlet column pressures are $P_i$ and $P_o$ respectively. For CCIGC, there is an insignificant pressure drop in the column and $j$ is approximately

unity. The $t_r' - t_c'$ is the dimensionless net retention time of the solvent as compared to an inert marker gas.

The net retention time can be calculated in different ways. If there is no diffusion resistance in the polymer, the elution peaks are perfectly symmetrical and the dimensionless time of the peak maximum, $t_{max}'$, gives the correct value of $t_r'$. However, diffusion is never infinitely fast in the polymer, and the elution peaks are never perfectly symmetrical. In this case, the dimensionless average solvent elution time called the dimensionless first moment ($\mu_1'$) should be used for $t_r'$ in order to relate the net retention time to purely thermodynamic properties. The dimensionless first moment is defined as

$$\mu_1' = \int_0^\infty t' C'(t')\, dt' = -\lim_{s\to\infty} \frac{dY}{ds} \tag{31}$$

Since eq 27 gives $Y(s)$ for an IGC experiment, the first moment can be derived by differentiating that expression according to eq 31.

$$\mu_1' = -\lim_{s\to\infty} \frac{dY}{ds} = \frac{2}{\alpha} + \epsilon + 1 \tag{32}$$

In the model derivations it was assumed that no pressure drop occurs in the column. Thus, the first moment from the model must be corrected by multiplying it by the $j$ factor. This multiplication corrects the theoretical moment so it is equivalent to the experimentally measured moment where pressure drop does occur. Substituting the first moment for ($jt_r'$) in eq 29 gives

$$V_g^0 = \frac{T_0}{T}\frac{L}{V}\frac{F}{M_p} j(t_r' - t_c') = \frac{T_0}{T}\frac{LA_c}{M_p}(\mu_1' - 1) \tag{33}$$

where $F = VA_c$.

Here, $A_c$ is the average cross sectional area of the vapor phase at any axial position in the column. Substitution for $\mu_1'$ gives

$$V_g^0 = \frac{T_0}{T}\frac{LA_c}{M_p}\left(\frac{K_p \tau A_s}{\chi} + \frac{K_s A_s}{\chi}\right) = \frac{T_0}{T}\frac{1}{M_p}(K_p V_p + K_s A_p) \tag{34}$$

In this equation, $V_p$ is the volume of polymer in the column, and $A_p$ is the exposed polymer surface area in the column. The partition coefficients are usually well represented by an Arrhenius temperature dependence.

$$K_p = K_p^0 \exp\left(\frac{-\Delta H_p}{RT}\right) \tag{35}$$

$$K_s = K_s^0 \exp\left(\frac{-\Delta H_s}{RT}\right) \tag{36}$$

Here, $K_p^0$ is a temperature independent preexponential factor and $\Delta H_p$ is the heat of absorption. Similar nomenclature is used for the surface adsorption partition coefficient. If both surface adsorption and bulk absorption significantly contribute to the retention volume, the retention diagram based on $\mu_1'$ will be nonlinear and monatonic (assuming both heats of sorption have the same sign). However, if one of the mechanisms dominates, the retention diagram based on $\mu_1'$ will be a straight line.

### Analysis of Retention Diagram When the Retention Volume Is Based on $t_{max}'$

Over the past several decades, numerous investigators have measured retention diagrams for different polymer−solvent systems.[1−7] While in some cases, the retention diagrams based on $t_{max}'$ were linear, many investigators have measured Z-shaped retention diagrams around the polymer glass transition temperature ($T_g$) as described in Figure 1. For example, Smidsrod and Guillet[1] found that when they injected different solvents (probe molecules) into a column packed with poly(*N*-isopropylacrylamide), this Z-shaped behavior often occurred. They also recognized that the first deviation from linearity on the right-hand side of the plot (lower temperatures) occurred fairly close to the $T_g$ of the polymer. Three of the probe solvents they used gave this behavior (hexadecane, α-chloronaphthalene, and naphthalene) while butyl alcohol and acetic acid gave a linear retention diagram. In their work, they used the time of the peak maximum ($t_{max}'$) to represent the retention time. They found that poor solvents for the polymer gave the Z-shaped behavior while good solvents did not. Further studies showed that good solvents sometimes gave the Z-shape.[3] Some investigators found that plasticized polymers did not give the Z-shape, while others found that they did.[5] So, the general conclusion was that IGC could sometimes be used to measure the polymer $T_g$ for reasons that were not well understood.

Braun and Guillet[9] proposed a model for this behavior suggesting that the retention volume could be formulated as a linear combination of adsorption and absorption mechanisms. They assumed that below the $T_g$, the solvent was not able to significantly penetrate the bulk polymer because the diffusion coefficient was too low. This would result in surface adsorption making the entire contribution to the retention volume. They argued that as the temperature increased, the diffusivity increased, and more of the bulk polymer was able to be penetrated. Their model was able to qualitatively predict the Z-shaped behavior using a depth penetration function that depended on temperature. To test their theory, the model derived above was used to determine the solvent concentration profile in the polymer coating. The goal was to see how the solvent penetrates the polymer when the diffusion coefficient is very low.

An IGC experiment was simulated using the model above by selecting nominal values for the dimensionless groups (α, $\beta$, $\gamma$, and $\epsilon$) below the $T_g$ of a polymer. A mutual binary diffusion coefficient of $1.0 \times 10^{-15}$ cm$^2$/s was chosen to represent a very low diffusion coefficient. The results of the simulation are shown in Figure 5. This plot shows the solvent concentration profile in the polymer coating at the column exit at different times when the diffusivity is very small.

Even when the diffusivity is extremely small, the solvent still penetrates the entire depth of the polymer sample. Thus, the theory put forth by Braun and Guillet provides a qualitative description of the Z-shaped retention diagram, but is flawed in the assumption about bulk diffusion below the glass transition temperature.

**Dependence of $t_{max}'$ on $D_p$.** To fully understand the origins of the Z-shaped retention diagram, it must first be understood how the polymer phase diffusion coef-

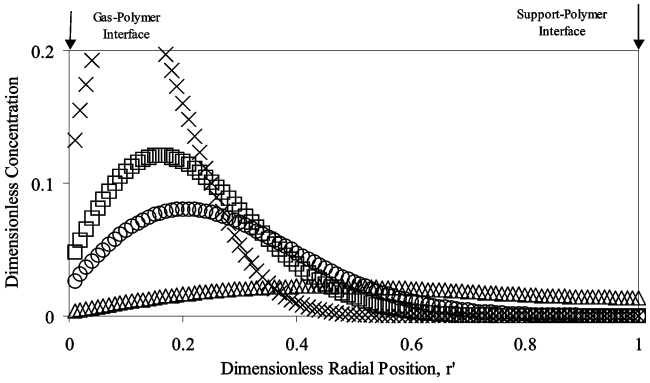


**Figure 5.** Solvent concentration profile in the polymer phase at the column exit when the polymer phase mutual diffusion coefficient is very low for $t' = 2$ (×), $t' = 3$ (□), $t' = 4$ (○), and $t' = 12$ (△).

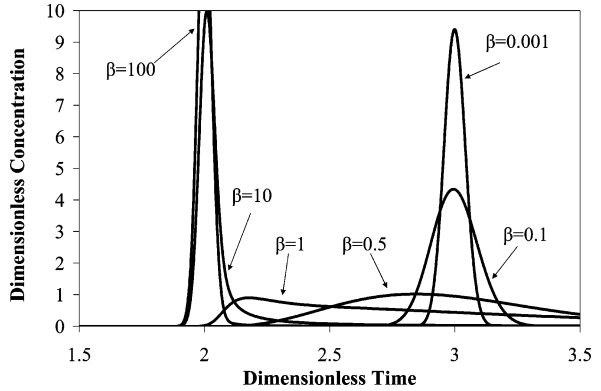


**Figure 6.** Effect of $\beta$ on the elution profile of an IGC experiment.

ficient ($D_p$) affects $t_{max}'$. To demonstrate this, the model derived above was used to simulate the elution profile for different values of the $\beta$ since it is the only parameter in the model that contains $D_p$. Simulating elution curves for different $\beta$ is equivalent to simulating the curves for different diffusion coefficients. The results of the simulations are shown in Figure 6.

In these simulations, the bulk sorption parameter, α was chosen to be 2.0. The surface adsorption parameter, $\epsilon$ was set to 1.0. The first moment of the peaks can be calculated from eq 32 to be: $\mu_1' = (2/\alpha) + \epsilon + 1 = 3$. The first moment is independent of $\beta$ and thus is the same for all of the curves. Visually, this may not appear to be true, but as $\beta$ gets large, the peaks become skewed and form long tails that are lost in the baseline. Three distinct regions can be identified in Figure 6.

The first region is when $\beta$ is very small. In this region, $D_p$ is large, the peaks are quite symmetrical, and $t_{max}'$ is equal to $\mu_1'$. The second distinct region appears when $\beta$ becomes very large. In this region, $D_p$ is very small and the peaks are extremely skewed, and even though $\mu_1'$ (the average dimensionless time of for probe molecule elution) is equal to 3, $t_{max}'$ approaches a limiting value of 2. If surface adsorption was the only mechanism of solvent retention (the solvent was insoluble in the bulk polymer), the value of $K_p$ would be zero and α would be infinity. In this limiting case, the first moment of the elution profile would be

$$\mu_1' = \frac{2}{\alpha} + \epsilon + 1 = \frac{2}{\infty} + \epsilon + 1 = \epsilon + 1 \quad \text{(no bulk absorption)} \quad (37)$$

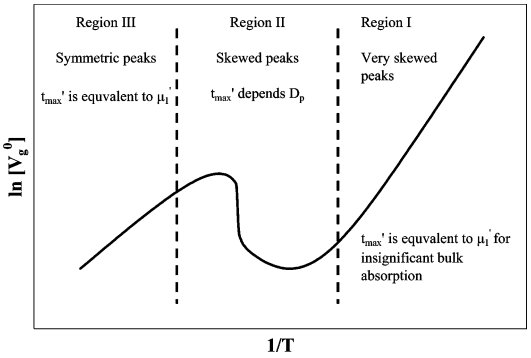


**Figure 7.** Critical regions of the Z-shaped retention diagram when the retention volume is based on $t_{max}'$.

For Figure 6, $\epsilon$ was set equal to 1. Substituting this value into eq 37 gives $\mu_1' = \epsilon + 1 = 2$. When $\beta$ becomes very large, $t_{max}'$ approaches this limiting value of 2. Thus, when the diffusion coefficient becomes very low, $t_{max}'$ is only characteristic of surface adsorption and contains no information about bulk absorption. This is not to say that bulk diffusion is not occurring, as it has been shown that bulk absorption occurs even when $D_p$ is very small. Instead, $t_{max}'$ simply loses all bulk sorption information in this limit. The third distinct region of Figure 6 lies between the first two regions when $\beta$ is not very small or very large. In this region, $t_{max}'$ depends on the value of $\beta$ and cannot be related to $\mu_1'$.

**Important Regions of the Z-Shaped Retention Diagram.** On the basis of these regions, a theory can be formulated to describe the Z-shaped retention diagram. The three regions of Figure 6 can be translated to the example Z-shaped retention diagram shown in Figure 1. This translation is shown in Figure 7.

$D_p$ always increases with increasing temperature. This means that $\beta$ will always decrease as the temperature is increased. The Z-shaped retention diagram is linear at low temperatures corresponding to very large $\beta$ (very small $D_p$). This linear portion of the retention diagram will be referred to as region I. In region I, $t_{max}'$ is equivalent to the limiting value of the first moment $\mu_1' = \epsilon + 1$ as described above. At high temperatures, the $D_p$ is very large and $\beta$ is very small. This portion of the retention diagram will be referred to as region III. In region III, $t_{max}'$ is equivalent to the true first moment $\mu_1' = (2/\alpha) + \epsilon + 1$. Finally, region II corresponds to the middle of the Z-shaped retention diagram. In region II, $t_{max}'$ depends on the value of $\beta$ and is not uniquely related to $\mu_1'$.

**Obtaining Model Parameters from an Experimental Z-Shaped Retention Diagram Based on $t_{max}'$.** From the definitions of the three regions, a procedure can be developed to obtain the model parameters (α, $\beta$, and $\epsilon$) from an experimental Z-shaped retention diagram based on $t_{max}'$. When based on $t_{max}'$, the retention volume in region I only depends on $\epsilon$. Since $\epsilon$ contains the surface adsorption partition coefficient ($K_s$) in its numerator, it is expected that $\epsilon$ will have Arrhenius temperature dependence.

$$\epsilon = \epsilon_0 \exp\left(-\frac{\Delta H_s}{RT}\right) \quad (38)$$

Here, $\epsilon_0$ is defined as $(A_s K_{s0}/\chi)$ (from eq 25) and $\Delta H_s$ is the heat of adsorption. In region I, $t_{max}'$ is equivalent to

the first moment in the limiting case when the solvent is insoluble in the bulk polymer.

$$\mu_1' = 1 + \epsilon = t_r' \tag{39}$$

Substituting this result into the expression for the specific retention volume gives

$$V_g^0 = \frac{T_0}{T}\frac{\chi}{\rho_p(1-\chi)}\epsilon \tag{40}$$

Here, the polymer mass and void volume have been written in terms of the polymer density and the column void fraction. This is a useful form since packed columns have a void fraction of about 0.5 for spherical packing. Under this assumption, the retention volume for a packed column in region I is approximately

$$V_g^0 = \frac{T_0}{T}\frac{\epsilon}{\rho_p} \tag{41}$$

Substitution of eq 38 gives

$$\ln\left[V_g^0\frac{T}{T_0}\rho_p\right] = \left(\frac{1}{T}\right)\left(\frac{-\Delta H_s}{R}\right) + \ln(\epsilon_0) \tag{42}$$

A plot of the left-hand side of eq 42 vs $1/T$ should be linear in region I. The slope of the line gives the heat of adsorption and the intercept gives $\epsilon_0$.

When based on $t_{max}'$, the retention volume in region III only depends on $\alpha$ and $\epsilon$. Since $\alpha$ contains the bulk sorption partition coefficient ($K_p$) in the denominator, its temperature dependence is expected to be

$$\alpha = \alpha_0 \exp\left(\frac{\Delta H_p}{RT}\right) \tag{43}$$

In this equation, $\alpha_0$ is defined as $(2\chi/\tau A_s K_{p0})$ and $\Delta H_p$ is the heat of absorption. In region III, the peak maximum is represented by the true first moment of the elution profile:

$$\mu_1' = \frac{2}{\alpha} + \epsilon + 1 = t_r' \tag{44}$$

Substituting this result for the retention time gives an expression for the retention volume in region III:

$$\ln\left[V_g^0\frac{T}{T_0}\rho_p - \epsilon\right] = \left(\frac{1}{T}\right)\left(\frac{-\Delta H_p}{R}\right) + \ln\left(\frac{2}{\alpha_0}\right) \tag{45}$$

Since the $\epsilon$ temperature dependence is known from region I, the left side of eq 45 can be plotted vs $1/T$. The slope of the line will give the heat of absorption and the intercept will give $\alpha_0$. Once $\epsilon$ and $\alpha$ are known functions of temperature, data in region II can be used to obtain the temperature dependence of $\beta$. Here, it is assumed that $D_p$ is an Arrhenius function of temperature over the temperature range of region II. Thus, $D_p$ and $\beta$ have the temperature dependencies of

$$D_p = D_{p0}\exp\left(-\frac{E}{RT}\right) \tag{46}$$

$$\beta = \beta_0\sqrt{\exp\left(\frac{E}{RT}\right)} \tag{47}$$

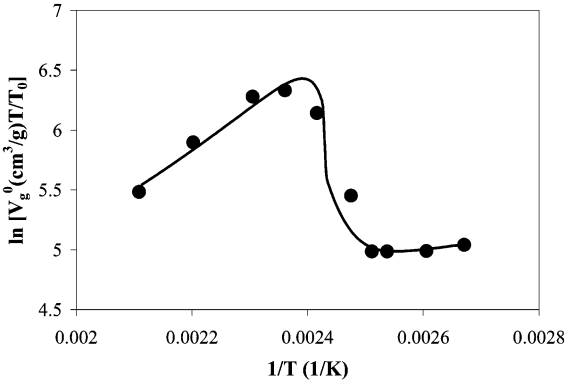


**Figure 8.** Model fit (solid line) of retention diagram for α-chloronaphthalene-poly(*N*-isopropylacrylamide). Experimental data (●) were taken from Smidsrod and Guillet.[1]

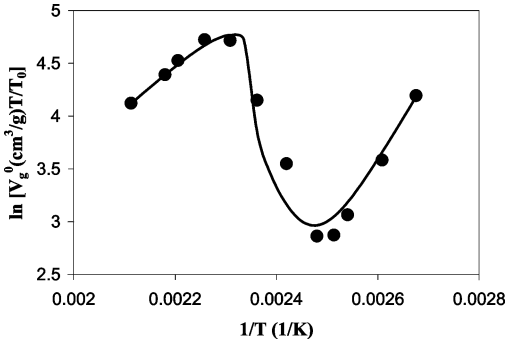


**Figure 9.** Model fit (solid line) of retention diagram for hexadecane-poly(*N*-isopropylacrylamide). Experimental data (●) were taken from Smidsrod and Guillet.[1]

Here, $\beta_0$ is defined as $\sqrt{(V\tau^2/LD_{p0})}$ and $E$ is the activation energy of diffusion. Three parameters ($\alpha$, $\beta$, and $\epsilon$) are needed for the model to predict the value of $t_{max}'$. If two of the three parameters are known somehow, the third parameter can be obtained by adjusting it until the model prediction of $t_{max}'$ matches the experimental value of $t_{max}'$. In this case, $\alpha$ and $\epsilon$ are known functions of temperature from experimental data collected in regions I and III. Thus, the value of $\beta$ can be determined for each experimental data point in region II by adjusting $\beta$ until the model prediction of $t_{max}'$ matches the experimental value of $t_{max}'$. Once $\beta$ has been calculated for each experimental data point in region II, $\beta_0$ and $E$ parameters can be obtained by linear regression of these $\beta$-temperature data according to eq 47.

Arrhenius temperature dependencies have been chosen to represent the partition and diffusion coefficients. It should be pointed out that this is only an approximation. Polymer solution diffusion coefficients are not expected to have Arrhenius temperature dependencies near the $T_g$. Here it is assumed that the $D_p$ is roughly Arrhenius over the small temperature range which $D_p$ affects $t_{max}'$ (region II). This assumption is further justified in the next section. Additionally, all model parameters should be expected to encounter some sort of transition around the $T_g$, but that has also been neglected in this simplified analysis.

**Model Correlation of Experimental Z-Shaped Retention Diagrams.** Experimental Z-shaped retention diagrams based on $t_{max}'$ that have been reported in the literature were correlated according to the procedure outlined above. Figures 8 and 9 show the results of this analysis on PCIGC data taken by Smidsrod and Guillet[1] for hexadecane and α-chloronaphtha-

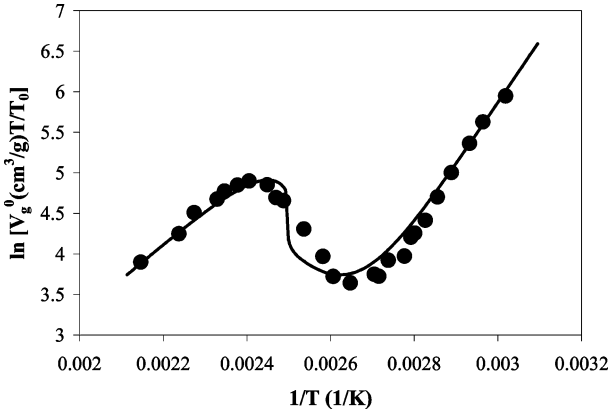


**Figure 10.** Model fit (solid line) of retention diagram for *n*-dodecane-polystyrene. Experimental data (●) were taken from Lavoie and Guillet.[2]

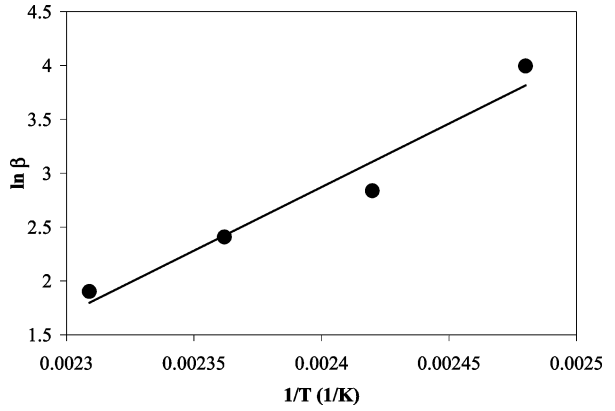


**Figure 11.** Arrhenius fit (solid line) of the diffusion coefficient ($\beta$) (●) in region II of the retention diagram for hexadecane−poly(*N*-isopropylacrylamide).

lene with poly(*N*-isopropylacrylamide). Figure 10 shows the model fit of PCIGC data taken by Lavoie and Guillet[2] for *n*-dodecane and polystyrene.

In all cases, the model gives a good correlation of the experimental retention volume data. The fit could be improved by invoking more complicated models for the temperature dependence of the $K_p$, $K_s$, and $D_p$. As mentioned in the previous section, $D_p$ is assumed to have an Arrhenius temperature dependence. This assumption can be verified by plotting ln $\beta$ vs $1/T$ in region II. Figure 11 shows this plot for the hexadecane-poly(*N*-isopropylacrylamide) data of Smidsrod and Guillet.[1]

## Measuring the Glass Transition Temperature from a Retention Diagram Based on $t_{max}'$

The glass transition temperature of the polymer does not appear in this new model for the Z-shaped retention diagram suggesting there is little correlation with $T_g$ and the Z-shaped retention diagram. The Z-shaped retention diagram is simply the transition between two regions where $t_{max}'$ is independent of the value of $D_p$. The only time that the first deviation from linearity occurs at the $T_g$ is when the value of the $D_p$ at the $T_g$ becomes large enough to significantly affect $t_{max}'$. Thus, it should be concluded that IGC cannot be used to determine the $T_g$ of a polymer by this technique. It is coincidental that in some cases the first deviation from linearity occurs near $T_g$. To better demonstrate this point, consider an arbitrary polymer solvent system. The thermodynamics and mass transport in such a system are described by the mutual binary diffusion coefficient, bulk partition coefficient, and the surface adsorption partition coefficient. Here it is assumed that these three parameters are Arrhenius functions of temperature, and the values of the Arrhenius correlation parameters for this arbitrary system are given in Table 2. Because it is assumed that all parameters are Arrhenius functions of temperature, this theoretical polymer has no glass transition. Thus, there should be no Z-shaped retention diagram as described by Braun and Guillet.

Let us assume that a packed column is constructed using this arbitrary polymer. The polymer is coated onto inert support particles that have a radius of 50 $\mu$m. The coating thickness on the particles is 1 $\mu$m. The column is 500 cm long, and experiments are conducted at a carrier gas velocity of 10 cm/s. Experiments are carried out at different temperatures ranging from 120 to 225 °C. The resulting retention diagram based on $t_{max}'$ is given in Figure 12. This diagram was created by model simulation for these prescribed conditions.

It has been argued that the glass transition temperature is not necessarily the temperature of the first deviation from linearity on the low-temperature portion of the retention diagram. The polymer simulated in Figure 12 had no glass transition yet gave the Z-shaped retention diagram with the first deviation from linearity occurring near 144 °C, demonstrating the flaw in this technique. Additionally, for any arbitrary polymer, like the one selected for this simulation, the $T_g$ is a constant and should not depend on the solvent probe, carrier gas velocity, particle radius, coating thickness, or any other experiment-dependent parameter. To test this idea, hypothetical packed column experiments were conducted on the same polymer−solvent system over the same range of temperatures, except at different carrier gas velocities. The retention diagrams based on $t_{max}'$ for each of these hypothetical experiments were simulated using the model. The resulting diagrams are shown in Figure 13.

Depending on the experimental conditions chosen, the first deviation from linearity will occur at different temperatures. In fact, for the simulated experiments above, the first temperature of linear deviation varied over a range of 40 °C. Thus, it is concluded that IGC should not be used to measure the $T_g$ of a polymer by this technique, as it is extremely dependent upon the experimental setup.

## Analysis of Retention Diagram when the Retention Volume is Based on the First Moment

Macris[8] and Arnould[10] argued that the retention volume should not be based on the $t_{max}'$, but on the first moment ($\mu_1'$) of the elution profile because they recognized that $t_{max}'$ depended upon the diffusion resistance in the polymer phase. If the first moment is used for the net retention time, then the retention volume will be given by eq 34. If calculated in this way, the retention volume should only depend on the thermodynamic partition coefficients and be independent of $\beta$. Arnould[10] tested this theory by collecting CCIGC data for different polymer solvent systems and calculated the retention volume by both $t_{max}'$ and $\mu_1'$. He found that, for all systems tested, the retention diagram based on $\mu_1'$ was linear over the entire temperature range (including the glass transition temperature) while the retention volume based on $t_{max}'$ gave the Z-shaped retention diagram. On the basis of these findings, he concluded that bulk absorption was the only dominant retention mechanism,

**Table 1. Parameters Obtained from $t_{max}'$-Based Retention Diagrams for Model Fits in Figures 8−10**

| parameter | system: α-chloronaphthalene−poly(*N*-isopropylacrylamide) | system: hexadecane−poly(*N*-isopropylacrylamide) | system: *n*-dodecane−polystyrene |
|---|---|---|---|
| $\alpha_0$ | 231.1 | 197.7 | 466.9 |
| $\Delta H_p$ (kcal/mol) | −9.2 | −8.2 | −8.6 |
| $\epsilon_0$ | 19.0 | $2.3 \times 10^{-08}$ | $3.2 \times 10^{-08}$ |
| $\Delta H_s$ (kcal/mol) | −1.6 | −16.1 | −15.3 |
| $\beta_0$ | $9.9 \times 10^{-20}$ | $8.9 \times 10^{-12}$ | $8.6 \times 10^{-08}$ |
| $E$ (kcal/mol) | 76.6 | 46.9 | 29.9 |

**Table 2. Arrhenius Coefficients for an Arbitrary Polymer−Solvent System**

| | |
|---|---|
| $K_{p0}$ | 0.2 |
| $\Delta H_p$ (kcal/mol) | −10 |
| $K_{s0}$ (cm) | $3 \times 10^{-11}$ |
| $\Delta H_s$ (kcal/mol) | −20 |
| $D_{p0}$ (cm$^2$/s) | $2 \times 10^{12}$ |
| $E$ (kcal/mol) | 50 |

and the Z-shaped diagram was simply an artifact of using the $t_{max}'$ analysis technique. It has been shown above that both bulk absorption and surface adsorption are significant retention mechanisms, so it is necessary to consider why surface absorption made an insignificant contribution to the retention time in his experiments. Using the data analysis technique described in the previous section, a set of PMMA-methanol $t_{max}'$ data collected by Arnould[10] was analyzed. These data were collected using an 18 m PMMA-coated capillary column. The coating thickness was about 3.7 $\mu$m. The temperature dependence of the $\epsilon$ and α parameters was found

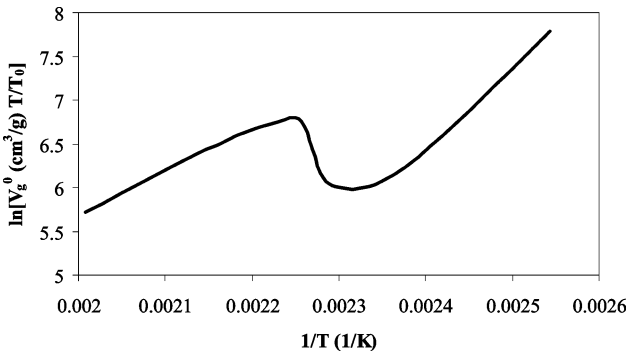


**Figure 12.** Simulated retention diagram for packed column experiments on an arbitrary polymer−solvent system whose characteristic parameters are given in Table 2. For this simulation, $\tau = 1$ $\mu$m, $L = 500$ cm, $V = 10$ cm/s, and $R = 50$ $\mu$m.

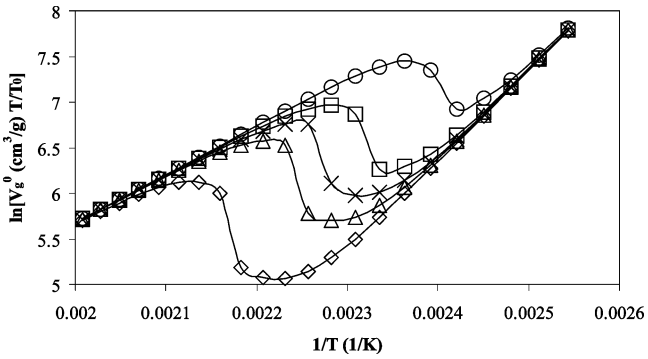


**Figure 13.** Simulated retention diagrams for packed column experiments on an arbitrary polymer−solvent system whose characteristic parameters are given in Table 2. For this simulation, $\tau = 1$ $\mu$m, $L = 500$ cm, and $R = 50$ $\mu$m. The different symbols represent different carrier gas velocities: 1 (○), 5 (□), 10 (×), 20 (△), and 100 cm/s (◇).

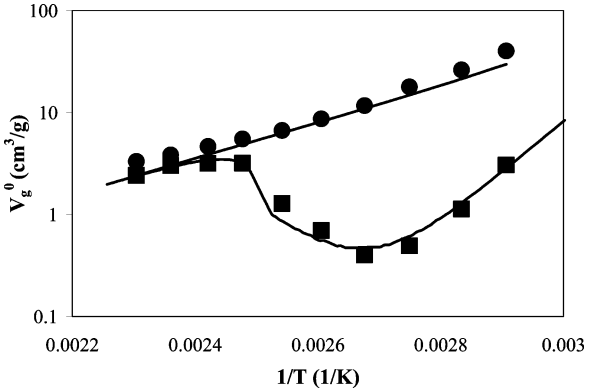


**Figure 14.** Model prediction of retention volume based on the first moment for PMMA-methanol. CCIGC data taken from Arnould[10]. First moment data (●) and $t_{max}'$ data (■) are shown along with the model predictions/fits (solid lines).

**Table 3. Parameters Obtained from Peak Maximum Retention Data for Model Fits in Figure 14**

| parameter | system: PMMA−methanol |
|---|---|
| $\alpha_0$ | $8.1 \times 10^4$ |
| $\Delta H_p$ (kcal/mol) | −7.3 |
| $\epsilon_0$ | $7.7 \times 10^{-16}$ |
| $\Delta H_s$ (kcal/mol) | −22.3 |
| $\beta_0$ | $7.8 \times 10^{-13}$ |
| $E$ (kcal/mol) | 43.0 |

from regions I and III of the $t_{max}'$ based retention diagram. Once $\epsilon$ and α were known, $\mu_1'$ was predicted by eq 32. Since Arnould also reported $\mu_1'$ based retention data, the first moment retention data predicted by the model can be compared to the experimentally determined first moment retention data. The model prediction of the retention volume as based on the first moment was found by eqs 32 and 33 while Arnould measured these retention data by numerical integration of his elution profiles. The results of this analysis are shown in Figure 14.

The $\mu_1'$-based retention diagram is accurately predicted from the α and $\epsilon$ obtained from the $t_{max}'$ based retention diagram. In this case, the $\mu_1'$-based retention diagram is linear because $\epsilon$ makes less than a 10% contribution to the first moment. However, this is not always true. Packed columns have a much larger surface-to-volume ratio than capillary columns, and thus $\epsilon$ could be expected to make a much larger contribution to the first moment in a packed column. However, in general, when the retention diagram is based on the first moment, it is rather insensitive to surface adsorption while the $t_{max}'$-based retention diagram is exceptionally sensitive to surface adsorption, especially in regions I and II. Because of this, it is probably less desirable to base the retention volume on the first moment because much more thermodynamic information can be gained by basing it on the $t_{max}'$.

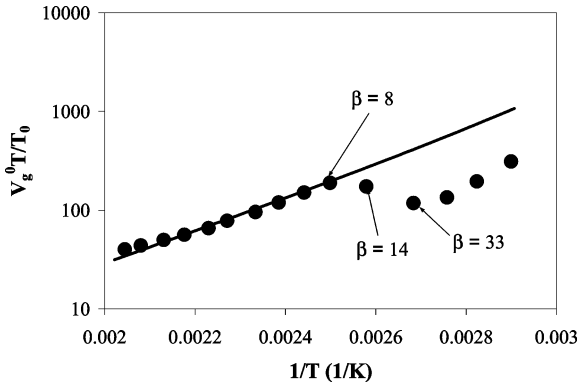


**Figure 15.** Model prediction (solid line) for the retention diagram of PS-*n*-decane based on the first moment. Experimental data (●) were taken from Panda et al.[2]

**Table 4. Parameters Obtained from Peak Maximum Retention Data for Model Fits in Figure 15**

| parameter | system PS−*n*-decane |
|---|---|
| $\alpha_0$ | 30.6 |
| $\Delta H_p$ (kcal/mol) | −6.3 |
| $\epsilon_0$ | $6.2 \times 10^{-6}$ |
| $\Delta H_s$ (kcal/mol) | −12.1 |
| $\beta_0$ | $3.2 \times 10^{-08}$ |
| $E$ (kcal/mol) | 30.5 |

However, if it is desired to neglect surface adsorption in data analysis and only consider bulk absorption, the retention volume should be based on the first moment.

In recent years, it has been found that even when based on the first moment, the retention diagram sometimes still takes on the Z-shape form. Panda et al.[7] found that PCIGC data for PMMA−benzene, PS−*n*-decane, and PMMA−*n*-decane all gave Z-shaped retention diagrams with both moment and peak maximum analysis. To study this further, the same analysis described above for Arnould's PMMA−methanol data was used to analyze the PS−*n*-decane data of Panda et al. Regions I−III of the $t_{max}'$-based retention diagram were used to find the temperature dependence of α, $\beta$, and $\epsilon$. These parameters were then used to predict the retention diagram as based on the first moment. The results of this analysis are shown in Figure 15.

The model predicts that the retention diagram should be linear when based on the first moment. However, the experimental retention diagram gives the Z-shaped form that would be expected if it were based upon $t_{max}'$. To understand why this happens, consider how the first moment is calculated from an experimental elution curve. The first moment was measured by Panda et al.[7] by numerical integration of the elution profile as given in eq 31. However, a problem exists when analyzing data in this manner. Observation of Figure 6 shows that as $\beta$ becomes large, the elution peaks become extremely skewed. This results in a sharp leading edge and a very long tail. The solvent concentration in the tailing region is quite low and gets lost in the baseline noise of the signal. Arnould[10] reported having difficulty integrating peaks of $\beta$ greater than 5 when α was equal to 0.2. As can be seen from Figure 15, the last point to fall on the linear portion of the retention diagram has a $\beta$ value of 8. The first point off of the linear portion has a $\beta$ value of 14. Elution peaks with $\beta$ values this large have long tails, and the deviation from the linear portion of the retention diagram suggests that the numerical integration underestimates the area due to a significant tail near the baseline. Therefore, it is concluded that if the retention diagram has a Z-shape when it is based on the first moment, it is likely that this is an artifact due to an inaccuracy of the numerical integration of the experimental data.

## Summary and Conclusions

A new model has been developed for binary polymer−solvent inverse gas chromatography experiments. The model has been generalized for either packed column or capillary column operation. Also, the model has been written to incorporate both bulk absorption in the polymer and surface adsorption on the gas−polymer interface. This new model has been used to better understand the Z-shaped retention behavior near the polymer glass transition temperature that has been reported over the last 45 years. Two ways have been demonstrated in which the retention volume can be determined: from the time of the peak maximum ($t_{max}'$) and from the first moment ($\mu_1'$) of the elution profile. Both of these techniques have been shown to be useful in obtaining thermodynamic and mass transfer information for polymer−solvent systems. When based on $t_{max}'$, the Z-shaped retention diagram is due to the effect of the polymer phase mutual binary diffusion coefficient ($D_p$) on the time of the peak maximum. This curve cannot in general be used to measure the $T_g$ of a polymer. This will only succeed if the diffusion coefficient at the $T_g$ is coincidentally the same value of the diffusion coefficient that begins to affect the $t_{max}'$. The Z-shaped behavior should not be observed if the first moment is used to calculate the retention diagram. Unless surface adsorption makes a significant contribution to the first moment, the retention diagram based on $\mu_1'$ will be linear. If the Z-shaped retention diagram appears when the retention volume is based on the first moment, this is probably due to the inability to accurately numerically integrate the elution profile when the peaks have long tails.

## Nomenclature

| | |
|---|---|
| $A_p$ | total surface area of polymer in column ($cm^2$) |
| $A_s$ | exposed polymer surface area in column per volume of empty column |
| $C$ | mass concentration of solvent in gas phase ($g/cm^3$) |
| $C'$ | dimensionless mass concentration of solvent in gas phase |
| $C_0$ | strength of the solvent injection ($g\ s/cm^3$) |
| $D_g$ | gas-phase diffusion coefficient ($cm^2/s$) |
| $D_p$ | mutual binary diffusion coefficient in polymer phase ($cm^2/s$) |
| $D_{p0}$ | preexponential factor for polymer phase diffusion coefficient ($cm^2/s$) |
| $E$ | activation energy of diffusion (J/mol) |
| $F$ | carrier gas flow rate ($cm^3/s$) |
| $\Delta H_p$ | heat of absorption (J/mol) |
| $\Delta H_s$ | heat of adsorption (J/mol) |
| $j$ | pressure drop correction factor |
| $K_p$ | bulk partition coefficient (dimensionless) |
| $K_p^0$ | preexponential factor for bulk sorption partition coefficient (dimensionless) |
| $K_s$ | surface adsorption partition coefficient (cm) |
| $K_s^0$ | preexponential factor for surface adsorption partition coefficient (cm) |
| $L$ | column length (cm) |

| | |
|---|---|
| $M_p$ | mass of polymer in the column (g) |
| $P_o$ | pressure at column outlet |
| $P_i$ | pressure at column inlet |
| $Q$ | Laplace domain dimensionless mass concentration of solvent in polymer phase |
| $R$ | radius of the gas−polymer interface or the support−polymer interface |
| $R$ | ideal gas constant (J/mol K) |
| $r$ | radial coordinate (cm) |
| $r'$ | dimensionless radial position |
| $s$ | Laplace domain independent variable |
| $T$ | column temperature (K) |
| $T_g$ | polymer's glass transition temperature |
| $T_0$ | reference temperature (K) |
| $t$ | time (s) |
| $t_c$ | retention time of an inert (s) |
| $t_r$ | retention time of solvent (s) |
| $t'$ | dimensionless time |
| $t_c'$ | dimensionless retention time of an inert (s) |
| $t_r'$ | dimensionless retention time of solvent (s) |
| $t_{max}'$ | dimensionless time of the elution peak maximum |
| $V$ | carrier gas velocity (cm/s) |
| $V_g^0$ | specific retention volume ($cm^3/g$) |
| $V_N$ | net retention volume ($cm^3/g$) |
| $V_p$ | volume of polymer in column ($cm^3$) |
| $Y$ | Laplace domain dimensionless mass concentration of solvent in gas phase |
| $z$ | axial position (cm) |
| $z'$ | dimensionless axial position (cm) |
| $\alpha$ | bulk absorption dimensionless group |
| $\beta$ | bulk diffusion dimensionless group |
| $\gamma$ | axial dispersion dimensionless group |
| $\delta$ | Dirac $\delta$ function |
| $\epsilon$ | surface adsorption dimensionless group |
| $\mu_1'$ | dimensionless first raw moment |
| $\rho$ | mass concentration of solvent in polymer ($g/cm^3$) |
| $\rho'$ | dimensionless mass concentration of solvent in polymer |
| $\chi$ | column void fraction |

**Acknowledgment.** This work was supported by the 3M Corp., Dow Chemical, and Air Products & Chemicals.

## References and Notes

(1) Smidsrod, O.; Guillet, J. E. *Macromolecules* **1968**, *2*, 272.
(2) Lavoie, A.; Guillet, J. E. *Macromolecules* **1969**, *2*, 443.
(3) Guillet, J. E.; Galin, M. *J. Polym. Sci., Part C: Polym. Lett.* **1973**, *11*, 233.
(4) Galassi, S.; Audisio, G. *Makromol. Chem.* **1974**, *175*, 2975.
(5) Braun, J. M.; Lavoie, A.; Guillet, J. E. *Macromolecules* **1975**, *8*, 311.
(6) Braun, J. M.; Guillet, J. E. *Macromolecules* **1976**, *9*, 340.
(7) Panda, S.; Bu, Q.; Huang, B.; Edwards, R. R.; Liao, Q.; Yun, K. S.; Parcher, J. F. *Anal. Chem.* **1997**, *69*, 2485.
(8) Macris, A. In *Chemical Engineering*; University of Massachusetts: Amherst, MA, 1979.
(9) Braun, J. M.; Guillet, J. E. *Macromolecules* **1976**, *9*, 617.
(10) Arnould, D. D. In *Chemical Engineering*; University of Massachusetts: Amherst, MA, 1989.
(11) Zielinski, J. M.; Duda, J. L. *AIChE J.* **1992**, *38*, 405.
(12) Laub, R. J.; Pecsok, R. L. *Physicochemical Applications of Gas Chromatography*; Wiley and Sons: New York, 1978.

MA0347767